ARTICLE

Spin-Unrestricted Multi-Configuration Time-Dependent Hartree Fock Theory

Wen-liang Li*, Ji-cheng Bian, Lei Yang

Key Laboratory at Universities of Education Department of Xinjiang Uygur Autonomous Region for New Energy Materials, Xinjiang Institute of Engineering, Urumqi 830091, China

(Dated: Received on October 29, 2013; Accepted on March 12, 2014)

Based on spin-unrestricted hartree fock theory, we present the spin unrestricted multi-configuration time dependent hartree fock theory (UMCTDHF) to describe the electron correlation dynamics of systems interacting with laser field. The positive spin orbitals and the negative spin orbitals are propagated in their own subspace respectively. The spin orbital in the spin-down subspace acts with that in the spin-up subspace by the reduced density matrix and mean field operator. The ground energy is acquired by propagating the trial wave function in the imaginary time by using spin-restricted MCTDHF (RMCTDHF) and UMCTDHF respectively. Then the ionization probabilities and the electrons energies are calculated by using RMCTDHF and UMCTDHF when the laser field is present. The ionization probability calculated with UMCTDHF agrees with the previous theoretical reports very well. The UMCTDHF method is accurate and applicable for open shell system beyond the capability of the RMCTDHF method.

Key words: Multi-configuration time dependent hartree fock theory, Electron-electron correlated, Strong laser field, Spin-unrestricted

I. INTRODUCTION

Over recent years, there has been increasing interest in the correlated dynamics of many-electrons systems [1−5]. A variety of explicit time-dependent versions of electronic structure methods have been developed, such as an important method known as multi-configuration time-dependent Hartree-Fock (MCTDHF) [6−13]. In 2003, Zanghellini *et al.* developed the MCTDHF method to deal with multi-electron dynamics in strong laser fields [6]. They showed that the MCTDHF method provided a good approximation of time-dependent multi-electron wave-functions [7] and was used to deal with the correlation of multi-electron system in strong laser fields [8]. In 2004, Kato *et al.* developed the theory in the second-quantization formalism [9, 10]. In 2005, Nest *et al.* developed the MCTDHF method by using atomic basis functions [11−14], following which they studied the electronically excited states of molecules [15] and ultrafast electron dynamics in LiH [16, 17] by using the MCTDHF method. The principle difference between the two versions is the difference in the type of basis function. Nest *et al.* used atomic basis functions in their theory [11−14] but Zanghellini *et al.* used grid vectors as the basis functions [6−8]. Recently, Birkeland *et al.* investigated the impact of the electron-electron correlation on the ionization dynamics of Helium in intense laser fields by solving time-dependent Schrödinger equation [18]. And Hochstuhl *et al.* studied the two-photo ionization of Helium with MCTDHF [19]. Recently, the time dependent ionization probabilities of Helium are calculated [20, 21]. The spin function is not explicit in the wave function and working equations. The spatial orbital of the spin-down function is the same as that of the spin-up function throughout the time when the wavefunction is propagated. We call the first option the RMCTDHF (R: restricted-spins) method. When the spatial orbital of the spin-down function is different from that of the spin-up function, we call that spin-unrestricted multi-configuration time-dependent Hartree Fock (UMCTDHF) method. In order to develop UMCTDHF method, two new sets of equations are derived exactly, and the spin orbital is divided into spin-down spaces and spin-up spaces. Each spin orbital is propagated in its own space.

In this work, we describes briefly the theory of UMCTDHF and demonstrates the test calculation on the helium atom. The results of RMCTDHF are also presented for comparison.

II. THEORY

We present an outline of UMCTDHF. Our notation follows closely the standard notation of the MCTDH

*Author to whom correspondence should be addressed. E-mail: wenliangli.dicp@gmail.com

method for nuclear quantum dynamics [20−24].

In UMCTDHF, the N-electrons wave-function can be linearly combined using time-dependent Slater determinants.

$$\begin{aligned}\Psi(\mathbf{x}_1,\mathbf{x}_2,\dots\mathbf{x}_N,t) &= \frac{1}{\sqrt{N!}}\sum_J A_J(t)|\chi_{j_1}(\mathbf{x}_1,t)\dots \\ &\quad \chi_{j_N}(\mathbf{x}_N,t)| \\ &= \frac{1}{\sqrt{N!}}\sum_J A_J(t)|J,t\rangle \end{aligned} \tag{1}$$

The capital letter J is a composite index which enumerates the N spin orbitals appearing in the determinant, and $\mathbf{x}_i$=($\mathbf{r}_i$, s_i) is a composite variable for the position $\mathbf{r}_i$ and the spin s_i. In the above equation the linear coefficients A_J and the spin orbitals $\chi_{j_1}(\mathbf{x}_1,t)$ are all assumed to be time-dependent, and $|\chi_1\chi_2\chi_3\rangle$ is an unrestricted Slater determinant.

The Hamiltonian describing the N electron system which interacts with the strong laser field:

$$H = \sum_{i=1}^{N}\frac{p_i^2}{2} + \sum_{i=1}^{N}V(r_i) + \sum_{i}^{N}\sum_{i>j}^{N}\frac{1}{r_{ij}} \tag{2}$$

The external potential $V(r_i)$ is produced by the (fixed) nuclei $V_{\rm nuc}(r_i)$ and may also contain the coupling to an additional laser field $V_{\rm exter}(r_i)$. With the aid of the variation principle one finds the following when varying the coefficients:

$$i\frac{\mathrm{d}A_J}{\mathrm{d}t} = \frac{1}{N!}\sum_L \langle J|H|L\rangle A_L \tag{3}$$

Variation with respect to the spin orbital $\chi_{i_1}(\mathbf{x}_1,t)$ yields

$$i\frac{\mathrm{d}\chi}{\mathrm{d}t} = (1-P)\frac{1}{\rho}\langle H\rangle\chi \tag{4}$$

$$P = \sum |\chi_i\rangle\langle\chi_i| = P_\alpha + P_\beta \tag{5}$$

$$\rho_{ij} = \left\langle \frac{\partial\Psi}{\partial\chi_i}\middle|\frac{\partial\Psi}{\partial\chi_j}\right\rangle \tag{6}$$

$$\langle H\rangle_{ij} = \left\langle \frac{\partial\Psi}{\partial\chi_i}\middle|H\middle|\frac{\partial\Psi}{\partial\chi_j}\right\rangle \tag{7}$$

where P is the projector operator on the total spin space spanned by all the spin orbital functions, ρ is the density operator, and $\langle H\rangle_{ij}$ is the so-called mean field operator.

We can obtain the motion equations of time dependent spatial orbital in α and β space respectively,

$$i\frac{\mathrm{d}\phi_\alpha}{\mathrm{d}t} = (1-P_\alpha)\frac{1}{\rho}\langle H\rangle\phi_\alpha \tag{8}$$

$$i\frac{\mathrm{d}\phi_\beta}{\mathrm{d}t} = (1-P_\beta)\frac{1}{\rho}\langle H\rangle\phi_\beta \tag{9}$$

It is important to emphasize here that the reduced density matrix and the mean field operator are also constructed in the total spin orbital spaces. Consequently, the two subspaces act with each other through the reduced density matrix and the mean field operator linking the spin-down subspace and spin-up space. Eqs. (3), (8) and (9) are the working equations of the UMCTDHF theory. These are similar to the relationships between the restricted spin Hartree Fock method and the unrestricted spin Hartree Fock (HF) method [25]. When the spatial orbital for the spin-down and spin-up subspaces are constrained to be the same, two sets of working Eq.(8) and Eq.(9) are reduced to one set equation.

III. RESULTS AND DISCUSSION

In order to test the validity of the UMCTDHF method, the imaginary time propagation and the real time propagation have been performed respectively. For simplicity, we take helium atom for example. Firstly, we calculate the ground state energy of the helium atom by propagating the initial wave function in imaginary time in the absence of the external laser field.

All our calculations have been done by using the orthogonal basis set. For a given number of spin orbitals M, there are C_M^N independent determinants. We employ the usual CASSCF notation CAS(N,M) to refer to a system with N electron and M spatial orbital for spin-down and spin-up space. The spin orbitals of spin-down and spin-up subspace are orthonormal to each other. However, the spatial orbital in the spin-down space is not orthonormal to that in the spin-up space.

The initial coefficients A_J are set to $N_s^{-1/2}$ for all possible unrestricted Slater determinants. The N_s is the number of Slater determinants. The initial spatial orbital was achieved by taking a Hartree Fock calculation. The HF calculations have been performed by using Molpro [26] or SMILES2007 [27, 28] basis set of avdz. The relaxation energies during the imaginary propagation time are plotted as a function of the propagation time as presented in Fig.1. By using RMCTDHF and UMCTDHF methods, we have increased the active space from 1 spatial orbital to 6 spatial orbitals. It is obvious that both of the results calculated by RMCTDHF with CAS(2,1) and that calculated by UMCTDHF with the same active space can reproduce the HF ground state energy perfectly. And the results of CAS(2,2), CAS(2,3), and CAS(2,6) for both methods are also shown. It can be found that with the increase of the spatial orbital, the results become much closer to the full configuration interaction energy (FCI) calculated by Molpro [24]. The relax energy of PIT with the number of 6 spatial orbitals is 2.8894 Hartree which is nearly equal to the FCI enegy 2.8895 Hartree of helium atom calculated by Molpro [24]. By comparing the calculated results of the RMCT-

DOI:10.1063/1674-0068/27/02/175-180

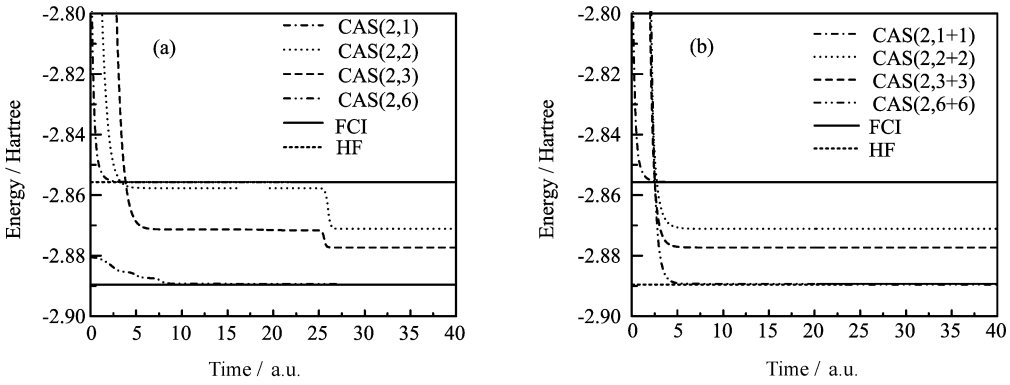

FIG. 1 Energy expectation values for the ground state of the helium atom calculated by using (a) RMCTDHF and (b) UMCTDHF.

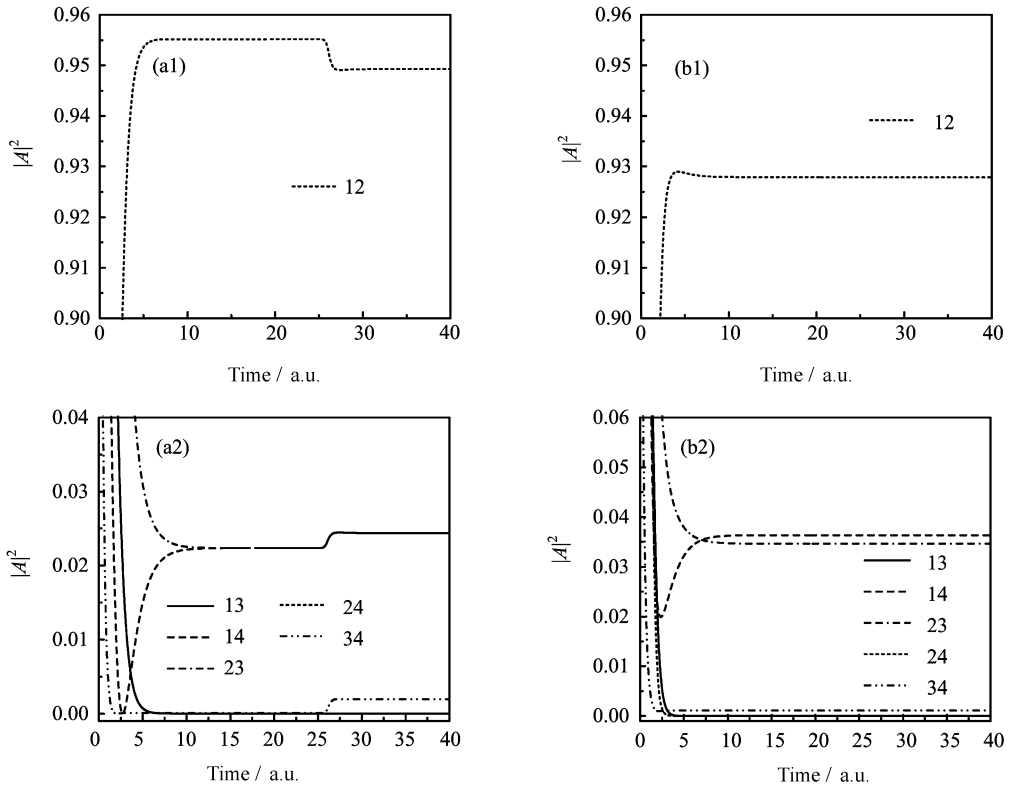

FIG. 2 The configuration components $|A^2|$ are plotted as a function of time. The results with CAS(2,2) are taken for example. (a) RMCTDHF, and (b) UMCTDHF. 1 represent the first spin orbital χ_1, 2 represent the second spin orbital χ_2, and 12 represent the configuration component $\chi_1\chi_2$, and so forth.

DHF and UMCTDHF with the same active spaces, we can find that the relax energy can reach the same energy value. But the relaxation processes of the RMCTDHF are different from that of UMCTDHF by propagating the same trial wavefucntion. We take CAS(2,2) for example. There are four spin orbitals χ_1=$\varphi_1\alpha$, χ_2=$\varphi_2\beta$, χ_3=$\varphi_3\alpha$, and χ_4=$\varphi_4\beta$ in the calculations. For RMCTDHF, the spatial part of spin orbital $\chi_1(\chi_3)$ is equal to that of spin orbital $\chi_2(\chi_4)$. For UMCTDHF, the spatial parts are different from each other. There are six configurations $\chi_1\chi_2$, $\chi_1\chi_3$, $\chi_1\chi_4$, $\chi_2\chi_3$, $\chi_2\chi_4$, and $\chi_3\chi_4$ available. The relaxed energy maintains steadily for a period times, and then relaxes the real ground state for RMCTDHF. For UMCTDHF, the energy relaxes the real ground state directly. In order to investigate in detail the underlying fundamental reasons for the different processes, the configuration components which are calculated by projecting the time-dependent wavefunction onto the available configurations are plotted as a function of the propagation time in Fig.2. From the results of the RMCTDHF (Fig.2(a)), it is clearly seen that the configuration components converge after about

DOI:10.1063/1674-0068/27/02/175-180

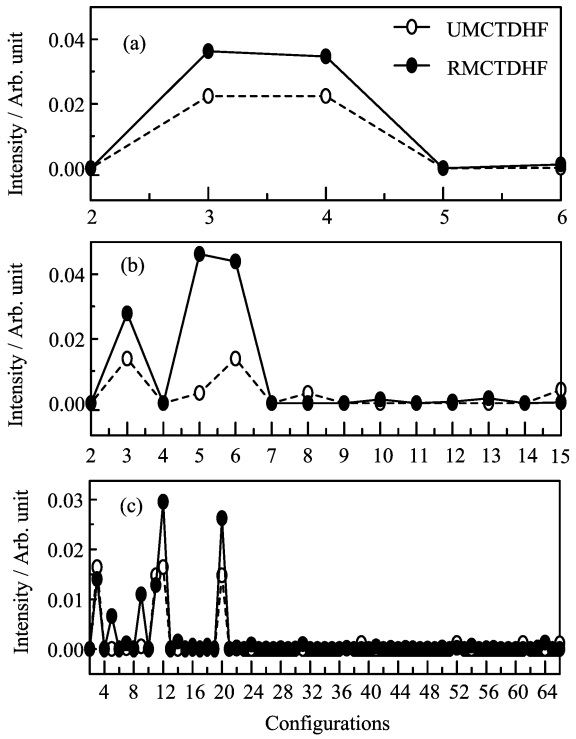

FIG. 3 The constitute of configuration components of RMCTDHF and UMCTDHF after the imaginary time propagation. (a) CAS(2,2), (b) CAS(2,3), and (c) CAS(2,6).

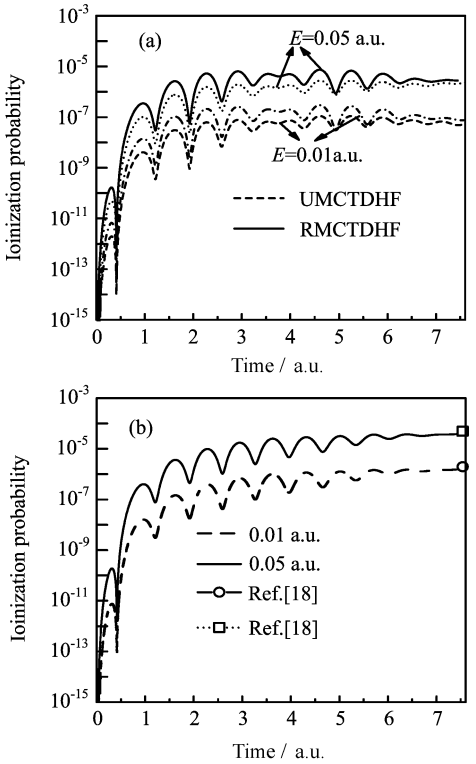

FIG. 4 The ionization probability are plotted as a function of time. (a) avdz and (b) 6-311G(2df,2pd).

10 a.u.. Then the component maintains steadily for a period of time, then varies at about 25 a.u. In addition to the relaxation process difference of RMCTDHF and UMCTDHF, the configuration components are also different from each other. When relaxation process ends, the configuration components are illustrated in Fig.3 for both RMCTDHF and UMCTDHF. The maximum values of configuration components in RMCTDHF calculations are 0.9552, 0.96213, and 0.93096 for CAS(2,2), CAS(2,3) and CAS(2,6) respectively. And while the maximum one calculated by UMCTDHF are 0.9279, 0.9552, 0.88885 respectively for CAS(2,2), CAS(2,3), CAS(2,6) which have 6, 15, 66 configurations respectively. It is obvious that the configuration component of UMCTDHF is different from that of RMCTDHF.

The real time propagation has been performed after the imaginary time propagation. The beginning wave function used in real time propagation is the ground state wave function with the CAS (2,6) for both RMCTDHF and UMCTDHF. The helium atom, which is prepared in the ground state, is exposed to a short, intense attosecond laser pulse. The field is linearly polarized and has a sine-squared temporal profile with ω=5 a.u. In the calculation, we take the same laser field as in Ref.[18]. We can calculate the ionization probability

$$\sigma = 1 - \sum_{i=1}^{N_{\text{state}}} \langle \Phi_i | \Psi(t) \rangle \tag{10}$$

where Φ_i is the bound state of the helium atom. By projecting the time-dependent wavefunction onto the bound states, the probability in the bound state can be achieved in the calculation. In Fig.4, we plot ionization probabilities as a function of propagation time for six-cycle pulses at laser frequency ω=5 a.u. by using basis set of avdz and 6-311G(2df,2pd) respectively. In Fig.4(a) the ionization probability calculated by UMCTDHF and RMCTOHF methods in different field strength, *i.e.* $E_{\max}$=0.01 and 0.05 a.u. are given. It is obvious that the calculated results of RMCTDHF are lower than that of UMCTDHF for both laser field $E_{\max}$=0.01 and 0.05 a.u. In Fig.4(b), only the results of UMCTDHF are presented, due to the similar trend to Fig.4(a). The ionization probabilities from Ref.[18] are shown by the points. It can be seen that the ionization probabilities used by basis set of 6-311G(2df,2pd) agree with the results taken from Ref.[18] very well. By comparing Fig.4 (a) and (b), we can get that the ionization probability calculated by RMCTDHF and UMCTDHF by using basis set of 6-311G(2df,2pd) are both higher than the results by using basis set of avdz. And the ionization probability with basis set of avdz is lower than the results from Ref.[18]. It may be due to that the number of basis set of 6-311G(2df,2pd) is bigger than that of avdz, it can describe well the time-dependent system wave-function when the laser filed is presented.

The energies of the electrons are plotted as a func-

DOI:10.1063/1674-0068/27/02/175-180

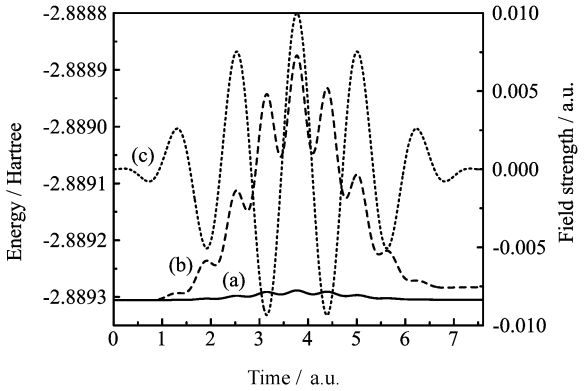

FIG. 5 The electron energies are calculated when the laser field with different maximum field strength is presented. (a) E=0.01 a.u. (b) E=0.05 a.u. (c) Laser field.

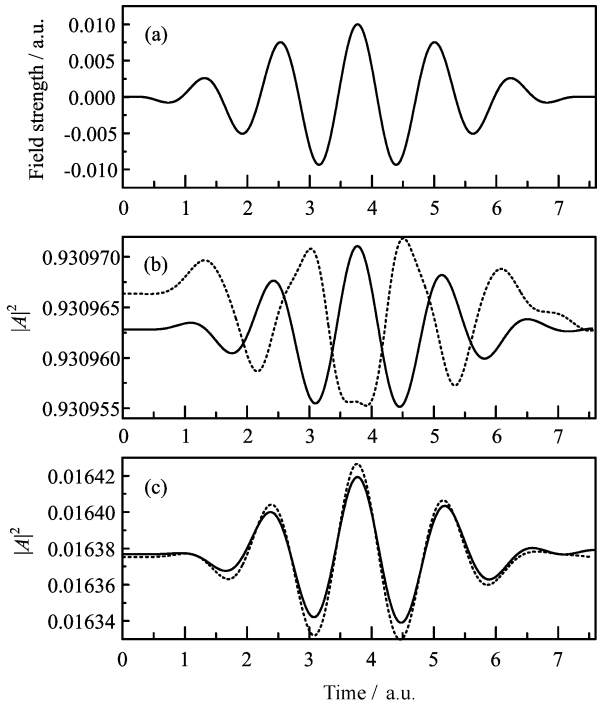

FIG. 6 The configuration components $\chi_1\chi_2$ and $\chi_1\chi_4$ are plotted as the real time when the laser field are present. (a) The laser field with $E_{\max}$=0.01 a.u., (b) and (c) are the configuration component for $\chi_1\chi_2$ and $\chi_1\chi_4$ respectively, solid line: UMCTDHF and dotted line: RMCTDHF.

tion of the time when laser field is present. As shown in Fig.5, it is obvious that the time-dependent electron energies with $E_{\max}$=0.05 a.u. is higher than that of $E_{\max}$=0.01 a.u. The electron energies calculated by RMCTDHF and UMCTDHF are nearly the same with the same laser field. When the laser field breaks off, the electron energy with UMCTDHF is lower than that of RMCTDHF. Both processes of RMCTDHF and UMCTDHF are nonadiabatic processes [29−31], the part ground state wavefunction goes to the excited state. The state of the interaction process is a mixed state with many components. We also want to know how the configuration component varies when the laser field varies. In Fig.6, the configuration component $\chi_1\chi_2$ and $\chi_1\chi_4$ are plotted as a function of the time. Figure 6(a) is the laser filed whose maximum laser strength $E_{\max}$=0.01 a.u. From Fig.6(b), we can see that the time-dependent configuration component of $\chi_1\chi_2$ in RMCTDHF is different from that of UMCTDHF. Figure 6(c) shows the variation of the configuration component $\chi_1\chi_4$. Both the configuration components of RMCTDHF and UMCTHDF display the same trends.

IV. CONCLUSION

An extended theoretical method based on unrestricted spin Hartree Fock theory, named UMCTDHF, is presented in this work. The total spin orbital space is divided into two subspaces (spin-down and spin-up subspaces). The time-dependent spin orbitals have been propagated in the two subspaces independently. The spin orbital in the spin-down subspace acts with the spin oribitals in the spin-up subspace by the common reduced density matrix and mean field operator, which are constructed in the total spin orbital space. Some illustrative calculations have been done. The ionization probabilities calculated by UMCTDHF agree with the latest theoretical results quantitatively. The UMCTDHF method is accurate and applicable for open shell system beyond the capability of the RMCTDHF method.

V. ACKNOWLEDGMENTS

This work was supported by the Scientific Research Program of the Higher Education Institution of Xinjiang, China (No.XJEDU2013S45).

[1] J. Hu, K. L. Han, and G. Z. He, Phys. Rev. Lett. **95**, 123001 (2005).
[2] L. Q. Feng, T. S. Chu, and L. Wang, Chin. Phys. B **22**, 023302 (2013).
[3] M. Y. Wu, Y. L. Wang, X. J. Liu, W. D. Li, X. L. Hao, and J. Chen, Chin. Phys. Lett. **30**, 073202 (2013).
[4] Y. Pan, S. F. Zhao, and X. X. Zhou, Phys. Rev. A **87**, 035805 (2013).
[5] S. L. Hu and T. Y. Shi, Chin. Phys. B **22**, 013101 (2013).
[6] J. Zanghellini, M. Kitzler, C. Fabian, T. Brabec, and A. Scrinzi, Laser Phys. **13**, 1064 (2003).
[7] J. Zanghellini, M. Kitzler, T. Brabec, B. Thomas, and A. Scrnzi, J. Phys. B **37**, 763 (2004).
[8] J. Caillat, J. Zhanghellini, M. Kitzler, O. Koch, W. Kreuzer, and A. Scrinzi, Phys. Rev. A **71**, 012712 (2005).

DOI:10.1063/1674-0068/27/02/175-180

[9] T. Kato and H. Kono, Chem. Phys. Lett. **392**, 533 (2004).
[10] T. Kato and K. Yamanouchi, J. Chem. Phys. **131**, 164118 (2009).
[11] M. Nest, T. Klamroth, and P. Saalfrank, J. Chem. Phys. **122**, 124102 (2005).
[12] M. Nest and T. Klamroth, Phys. Rev. A **72**, 012710 (2005).
[13] M. Nest, J. Theor. Comput. Chem. **6**, 563 (2007).
[14] M. Nest, J. Chem. Phys. **472**, 171 (2009).
[15] M. Nest, R. Padmanaban, and P. Saalfrank, J. Chem. Phys. **126**, 124106 (2007).
[16] F. Remacle, M. Nest, and R. D. Levine, Phys. Rev. Lett. **99**, 183902 (2007).
[17] M. Nest, F. Remacle, and R. D. Levine, New J. Phys. **10**, 025019 (2008).
[18] T. Birkeland, R. Nepstad, and M. Fore, Phys. Rev. Lett. **104**, 163002 (2010).
[19] D. Hochstuhl and M. Bonitz, J. Chem. Phys. **134**, 084106 (2011).
[20] W. L. Li and W. W. Xu, Mol. Phys. **111**, 119 (2013).
[21] W. L. Li, W. W. Xu, and T. S. Chu, Comput. Theor. Chem. **1004**, 18 (2013).
[22] H. D. Meyer, U. Manthe, and L. S. Cederbaum, Chem. Phys. Lett. **165**, 73 (1990).
[23] H. D. Meyer, U. Manthe, and L. S. Cederbaum, J. Chem. Phys. **97**, 3199 (1992).
[24] M. H. Beck, A. Jackle, G. A. Worth, and H. D. Meyer, Phys. Rep. **324**, 1 (2000).
[25] A. Szabo and N. S. Ostlund, *Modern Quantum Chemistry*, New York: Dover, (1996).
[26] H. J. Werner, P. J. Konwles, R. D. Amos, A. Berning, D. L. Cooper, M. J. Deegan, A. J. Dobbyn, F. Eckert, C. Hampel, T. Leininger, R. Lindh, A. W. Lloyd, W. Meyer, M. E. Mura, A. Nickla, P. Palmieri, K. Peterson, R. Pitzer, P. Pulay, G. Rauhut, M. Schfltz, H. Stoll, A. J. Stone, and T. Thoresteinsson, MOLPRO Version 2006.1, a Package of *ab initio* Programs, (2006), http://www.molpro.net/.
[27] R. J. Fernandez, R. Lopez, A. Aguado, I. Ema, and J. Ramirez, J. Comput. Chem. **19**, 1284 (1998).
[28] R. J. Fernandez, R. Lopez, A. Aguado, I. Ema, and J. Ramirez, Int. J. Quantum Chem. **81**, 148 (2001).
[29] T. S. Chu, Y. Zhang, and K. L. Han, Int. Rev. Phys. Chem. **25**, 201 (2006).
[30] T. S. Chu and K. L. Han, Phys. Chem. Chem. Phys. **10**, 2431 (2008)
[31] T. S. Chu and K. L. Han, J. Phys. Chem. A **109**, 2050 (2005).

DOI:10.1063/1674-0068/27/02/175-180